

Toward a tomographic picture of a Bose–Einstein condensate

Stefano Mancini

Istituto Nazionale per la Fisica della Materia, Dipartimento di Fisica, Università di Milano, Via Celoria 16, I-20133 Milan, Italy

Mauro Fortunato and Paolo Tombesi

Istituto Nazionale per la Fisica della Materia, Dipartimento di Matematica e Fisica, Università di Camerino, I-62032 Camerino, Italy

Giacomo Mauro D'Ariano

Istituto Nazionale per la Fisica della Materia, Dipartimento di Fisica "A. Volta," Università di Pavia, I-27100 Pavia, Italy

Received March 9, 2000; revised manuscript received September 12, 2000; accepted September 12, 2000

The possibilities of applying tomographic techniques to a Bose–Einstein condensate to reconstruct its ground state are investigated by means of numerical simulations. Two situations for which the density-matrix elements can be retrieved from atom counting probabilities are considered. The methods presented here allow one to distinguish among various possible quantum states. © 2000 Optical Society of America
[S0740-3232(00)03712-1]

OCIS codes: 270.0270, 010.0020.

1. INTRODUCTION

Even before the birth of quantum mechanics, optics and mechanics have long developed on parallel tracks, because light and massive entities were considered as waves and particles, respectively. At the beginning of the twentieth century, with the introduction of quantum mechanics, waves and particles started to play an interchangeable role, with the concepts of photons and of the de Broglie wavelength. This gave rise to the birth of quantum optics and atom optics.¹ However, while an optical single-mode system has been available since long ago, the same cannot be said for matter waves. In fact, in the field of atom optics, only recently have breakthroughs in the evaporative cooling of dilute alkali gases allowed the generation of Bose–Einstein condensates (BEC's).² The BEC is a macroscopic occupation of the ground state of the gas and is one important paradigm of quantum statistical mechanics.

In recent theoretical and experimental investigations of BEC's, one of the most important and urgent issues is the determination of the actual quantum state of the condensate. In fact, as in optics, the presence of many particles in a single mode makes it possible to explore the multiparticle quantum state of the mode. At first thought, a number state might seem a natural description of a condensate mode, but the actual state may well depend on the details of preparation. For example, both the demonstration of first-order interference³ and observations of normalized, spatial correlation functions⁴ near unity suggest coherent states, while the presence of collisions among atoms may lead to the formation of squeezed

states.⁵ Also, the internal states of the condensate atoms allow precise manipulation of the BEC state by interaction with light.⁶

Few experimental methods of obtaining partial information about the quantum state of a BEC have been suggested.⁷ However, motivated by the success of quantum tomographic techniques in optics,⁸ a number of researchers have recently proposed more-direct methods for measuring the quantum state of a BEC.^{9–11}

In optical tomography the key point is the use of a reference field, namely, the local oscillator.⁸ This device, prepared in a coherent state, allows one to probe the desired state through the measurement of a set of probabilities.¹² However, a difficulty arises if one tries to adapt the same technique to a BEC. In fact, while in optics it is easy to obtain a coherent reference field (e.g., from a laser), such a field is not actually available for atoms. Nevertheless, recent reports of progress in this direction seem promising.^{13,14} Hence, in the present paper, we provide a detailed study of the possibility of reconstructing the quantum state of a BEC with the inclusion of both situations: when a reference field is available and when it is not.

The paper is organized as follows. In Section 2 we review the tomographic principle and consider a suitable operator transform on the atomic system. In Section 3 we consider the case of state reconstruction in the absence of a reference field, and in Section 4 the opposite case is analyzed. Finally, in Section 5 we comment on the numerical results, and in Section 6 we conclude with a brief discussion.

2. BASIC MODEL

Recently, we established¹⁵ a very general principle for constructing measurable probabilities, which determine completely the quantum state in the tomographic approach. For a more refined treatment, see Ref. 16.

Let us consider a quantum state described by the density operator $\hat{\rho}$, which is a nonnegative Hermitian operator, i.e.,

$$\hat{\rho}^\dagger = \hat{\rho}, \quad \text{Tr } \hat{\rho} = 1, \quad (1)$$

$$\langle v | \hat{\rho} | v \rangle = \rho_{v,v} \geq 0. \quad (2)$$

We label the vector basis $|v\rangle$ in the space of pure quantum states by the index v , which may represent any degree of freedom of the system under consideration. Relation (2) can be rewritten by use of the Hermitian projection operator

$$\hat{\Pi}_v = |v\rangle\langle v| \quad (3)$$

in the following form:

$$\rho_{v,v} = \text{Tr}(\hat{\Pi}_v \hat{\rho}). \quad (4)$$

At the same time, in the space of states, there will be a family of unitary transformation operators $\hat{U}(\sigma)$ that depend on some parameters $\sigma = (\sigma_1, \dots, \sigma_k, \dots)$, which can sometimes be identified with a group-representation operator. It has been shown¹⁵ that known tomography schemes can be considered from the viewpoint of group theory by use of appropriate groups. More recently, this concept has been developed to yield an elegant group-theoretic approach to quantum state measurement.¹⁶ Here we formulate the tomographic approach in the following way. Let us introduce a transformed density operator

$$\hat{\rho}_\sigma = \hat{U}^{-1}(\sigma) \hat{\rho} \hat{U}(\sigma). \quad (5)$$

Its diagonal elements are still nonnegative probabilities:

$$\langle v | \hat{\rho}_\sigma | v \rangle = w(v, \sigma) \geq 0. \quad (6)$$

These probabilities are functions of stochastic variable(s) v and parameter(s) σ . As a consequence of the unit trace of the density operator, these probabilities also fulfill the normalization condition

$$\int dv w(v, \sigma) = 1. \quad (7)$$

Of course, in the case of discrete indices, the integral in Eq. (7) should be replaced by a sum over discrete variables.

The left-hand side of Eq. (6) can be interpreted as the probability density for the measurement of the observable \hat{V} (the operator whose eigenstates are given by $|v\rangle$) in an ensemble of transformed reference frames labeled by the index σ , provided that the state $\hat{\rho}$ is given. Along with this interpretation, one can also consider the transformed projector

$$\hat{\Pi}_v(\sigma) = \hat{U}(\sigma) \hat{\Pi}_v \hat{U}^{-1}(\sigma), \quad (8)$$

in terms of which Eq. (6) for the probability $w(v, \sigma)$ takes the form

$$w(v, \sigma) = \text{Tr}[\hat{\rho} \hat{\Pi}_v(\sigma)]. \quad (9)$$

These probability densities are also called marginal distributions as a generalization of the concept introduced by Wigner.¹⁷ The tomography schemes are based on the possibility of finding the inverse of Eq. (9). If it is possible to solve Eq. (9), considering the probability $w(v, \sigma)$ as a known function and the density matrix as an unknown operator, the quantum state can be reconstructed in terms of measurable positive-definite probability distributions. This is the essence of state reconstruction techniques.

Specifically, we consider two atomic sources whose atoms (described by two bosonic modes \hat{b}_1 and \hat{b}_2) can be mixed through an atomic beam splitter,¹⁸ we assume that a phase shift ϕ can also be introduced successively between them. We shall specify these modes below. At the output a detection of the number of atoms in both modes can be performed. This amounts to the possibility of measuring the probability distributions related to the transformed state

$$\hat{\rho} \rightarrow \hat{U}(\theta, \phi) \hat{\rho} \hat{U}^\dagger(\theta, \phi), \quad (10)$$

where the transformation operator is given by

$$\hat{U}(\theta, \phi) = \exp\{-i(\theta/2)[b_1^\dagger b_2 \exp(-i\phi) + b_1 b_2^\dagger \exp(i\phi)]\}. \quad (11)$$

Here, $\cos^2(\theta/2)$ represents the transmission coefficient at the beam splitter. Relation (10) plays the same role as Eq. (5), and, in the spirit of the tomographic principle, the set of marginals associated with the transformed state will allow us to recover the original state. In Sections 3 and 4, as anticipated in Section 1, we shall distinguish the two situations that involve the availability of a reference field.

3. CASE 1

We first treat the case in which a reference field is not available. All that we can do in this case is to consider two condensates that belong to the two modes \hat{b}_1 , \hat{b}_2 , imposing the constraint of total particle number conservation, i.e., $[\hat{\rho}, \hat{N}] = 0$, to infer their (joint) state. This state is assumed to be a generic two-mode state of the type

$$|\Psi\rangle = \sum_{n=0}^N c_n |N-n\rangle_1 |n\rangle_2. \quad (12)$$

At this stage we use the formal equivalence between the algebra for two harmonic oscillators and that for angular momentum.¹⁹ We write the state $|n\rangle_1 |N-m\rangle_2 = |j+m\rangle_1 |j-m\rangle_2$ as a spin state $|m\rangle$, where $j = N/2$ and $m = n - j$ ($m = -j, -j+1, \dots, j-1, j$). The $j+1$ states $|m\rangle$ have all the properties of the eigenstates of \hat{J}^2 and \hat{J}_z , where

$$\begin{aligned} \hat{J}_+ &= \hat{J}_-^\dagger = \hat{b}_1^\dagger \hat{b}_2, & \hat{J}_z &= (1/2)(\hat{b}_1^\dagger \hat{b}_1 - \hat{b}_2^\dagger \hat{b}_2), \\ \hat{J}^2 &= \hat{J}_z^2 + (1/2)(\hat{J}_+ \hat{J}_- + \hat{J}_- \hat{J}_+). \end{aligned} \quad (13)$$

The effect of the beam splitter, including the phase shift, is a rotation by an angle θ about an axis $\mathbf{u}_\phi = \mathbf{u}_x \cos \phi - \mathbf{u}_y \sin \phi$ of the angular momenta $\hat{\mathbf{J}}$, i.e.,

$$\hat{U}(\theta, \phi) = \exp(-i\theta\hat{\mathbf{J}} \cdot \mathbf{u}_\phi). \quad (14)$$

At the same time, the rotation (14) can be specified by means of the Wigner- D function¹⁹:

$$\langle m' | \hat{U}(\theta, \phi) | m \rangle \equiv \mathcal{D}_{m'm}^{(j)}(\psi = 0, \theta, \phi), \quad (15)$$

where now ψ, θ, ϕ represent the Euler angles. Then the probability of $j + m$ counts at the first detector, and $j - m$ at the second one is given by

$$w(m, \theta, \phi) = \sum_{m_1=-j}^j \sum_{m_2=-j}^j \mathcal{D}_{mm_1}^{(j)}(\psi, \theta, \phi) \rho_{m_1 m_2}^{(j)} \times \mathcal{D}_{mm_2}^{(j)*}(\psi, \theta, \phi). \quad (16)$$

The measurement of the atomic number in both modes guarantees a unit efficiency. In fact, data for which the sum of counts is not N can be disregarded. Moreover, in Eq. (16) we have left the argument ψ unspecified in the right-hand side and have omitted it in the left-hand side, since $\mathcal{D}_{mm'}^{(j)} \propto \exp(-im\psi)$: The marginal distribution depends only on the two angles θ and ϕ .

Following Refs. 20 and 21 we will derive the expression for the density matrix of a spin state in terms of measurable probability distributions. This can be done by use of the known integral product of three Wigner- D functions over the rotation group and with the orthogonality of the Wigner- $3j$ symbols $\mathcal{W}_{m_1 m_2 m_3}^{j_1 j_2 j_3}$.¹⁹ Finally, the density-matrix elements can be expressed in terms of the marginal distribution as

$$\begin{aligned} \rho_{m_1 m_2}^{(j)} &= (-1)^{m_2} \sum_{j'=0}^{2j} \sum_{m'=-j'}^{j'} (2j' + 1)^2 \\ &\times \sum_{m=-j}^j \int (-1)^m w(m, \theta, \phi) \\ &\times \mathcal{D}_{0m'}^{(j')}(\psi, \theta, \phi) \mathcal{W}_{m-m_0}^{jjj'} \mathcal{W}_{m_1-m_2 m'}^{jjj'} \frac{d\Omega}{8\pi^2}, \end{aligned} \quad (17)$$

where the integration is performed over the rotation parameters, i.e.,

$$\int d\Omega = \int_0^{2\pi} d\psi \int_0^\pi \sin\theta d\theta \int_0^{2\pi} d\phi. \quad (18)$$

Thus we can use Eq. (17) to sample two-mode BEC density-matrix elements, starting from the measurable probabilities $w(m, \theta, \phi)$ and some known functions.

4. CASE 2

Recent progress in the generation of an atomic coherent source¹³ makes us hopeful about the possibility of having an atomic reference field.¹⁴ Thus, in this section, we shall consider the first mode as the condensate to be investigated and the second mode as coming from a coherent atomic source.

Let $\hat{\rho}$ be the state of mode 1 that we wish to reconstruct and $\bar{\beta}$ the coherent state characterizing mode 2. Then the probability of counting n atoms in mode 1, for $\theta = \pi/2$, will be

$$w(n, \beta) = \text{Tr}[\hat{U}^{-1}(\theta = \pi/2, \phi) \hat{\rho} |\bar{\beta}\rangle_{22} \times \langle \bar{\beta} | \hat{U}(\theta = \pi/2, \phi) | n \rangle_{11} \langle n |], \quad (19)$$

where $\beta = |\bar{\beta}| \exp(i\varphi)$, $\varphi = \arg \bar{\beta} - \phi + (\pi/2)$. This corresponds to the probability distribution for the measurement of the displaced number operator $\hat{D}^\dagger(\beta) \hat{b}_1^\dagger \hat{b}_1 \hat{D}(\beta)$, analogously to what is done in photon number tomography.²² In photon number tomography, however, one has to collect number distributions by spanning the whole complex plane β ; here, instead, we will simplify the procedure (see also Ref. 23).

Of course, the number of atoms in the condensate, though not fixed, will be finite; thus it happens that $\langle k | \rho | m \rangle = 0$ for $k, m > N_1$, with N_1 being a suitable estimation of the maximum number of the condensed atoms. By virtue of this assumption we can rewrite Eq. (19) as

$$\begin{aligned} w(n, \beta) &= \exp(-|\beta|^2) n! \sum_{k,m=0}^{N_1} \langle k | \rho | m \rangle \\ &\times \frac{1}{\sqrt{k!m!}} |\beta|^{m+k-2n} \exp[i(m-k)\varphi] \\ &\times L_n^{(m-n)}(|\beta|^2) L_n^{(k-n)}(|\beta|^2), \end{aligned} \quad (20)$$

where $L_n^{(m)}$ are the associated Laguerre polynomials.

Let us now consider, for a given value of $|\beta|$, the function $w(n, \beta)$ as a function of φ and calculate the coefficients of the Fourier expansion, which are

$$w^{(s)}(n, |\beta|) = \frac{1}{2\pi} \int_0^{2\pi} d\varphi w(n, \beta) \exp(is\varphi) \quad (21)$$

($s = 0, 1, 2, \dots$). By combining Eqs. (20) and (21), we get

$$w^{(s)}(n, |\beta|) = \sum_{m=0}^{N_1-s} \mathcal{A}_{n,m}^{(s)}(|\beta|) \langle m+s | \rho | m \rangle, \quad (22)$$

where

$$\begin{aligned} \mathcal{A}_{n,m}^{(s)}(|\beta|) &= \exp(-|\beta|^2) n! \frac{1}{\sqrt{(m+s)!m!}} \\ &\times |\beta|^{2(m-n)+s} L_n^{(m-n)}(|\beta|^2) L_n^{(m+s-n)}(|\beta|^2). \end{aligned} \quad (23)$$

If the distribution $w(n, \beta)$ is measured for $n = 0, 1, \dots, N$ ($N \geq N_1$), then Eq. (22) represents, for each value of s , a system of $(N+1)$ linear equations between the $(N+1)$ measured quantities and the $(N_1 + 1 - s)$ unknown density-matrix elements. Therefore, to obtain the latter, we need only invert the system²⁴

$$\langle m+s | \rho | m \rangle = \sum_{n=0}^N \mathcal{M}_{m',n}^{(s)}(|\beta|) w^{(s)}(n, |\beta|), \quad (24)$$

where the matrices \mathcal{M} are given by $\mathcal{M} = (\mathcal{A}^T \mathcal{A})^{-1} \mathcal{A}^T$. It is possible to see that such matrices satisfy the relation

$$\sum_{n=0}^N \mathcal{M}_{m',n}^{(s)}(|\beta|) \mathcal{A}_{n,m}^{(s)}(|\beta|) = \delta_{m,m'}, \quad (25)$$

for $m, m' = 0, 1, \dots, N_1 - s$, which means that from the exact probabilities satisfying Eq. (22) the correct density matrix is obtained. By combining Eqs. (24) and (21) we find that

$$\langle m + s | \rho | m \rangle = \frac{1}{2\pi} \sum_{n=0}^N \int \hat{d}\varphi \mathcal{M}_{m,n}^{(s)}(|\beta|) \exp(is\varphi) w(n, \beta), \quad (26)$$

which may be regarded as the formula for the direct sampling of the condensate density matrix. In particular, we can see that the determination of the state of the condensate requires only that the value of φ (i.e., the phase between reference and condensate field) be varied. Moreover, the present reconstruction procedure involves Laguerre polynomials in place of additional summations, guaranteeing a better stability in the numerical manipulation of a large set of data, as compared with analogous methods.²³

Finally, the non-unit-efficiency η in the detection process can be accounted for by consideration of a binomial convolution of the ideal probability²⁵:

$$w_\eta(k, \beta) = \sum_{n=k}^{\infty} \binom{n}{k} \eta^k (1 - \eta)^{n-k} w(n, \beta), \quad (27)$$

with the consequent modification of the matrix \mathcal{A} .

5. NUMERICAL RESULTS

It is plausible, as has already been suggested,^{5,11} that the state of a condensate with repulsive collisions may be a squeezed state with reduced number fluctuations. Hence below we will consider this situation. A single one-mode state can be written as

$$|\Psi\rangle = \sum_{n=0}^{\infty} c_n |n\rangle, \quad (28)$$

where the coefficients c_n are given by²⁶

$$c_n = \left(\frac{2}{r+1} \right)^{1/2} r^{1/4} \left(\frac{r-1}{r+1} \right)^{n/2} (2^n n!)^{-1/2} H_n \times \left(\sqrt{\frac{2r^2}{r^2-1}} x_0 \right) \exp\left(-\frac{r}{r+1} x_0^2 \right), \quad (29)$$

where r is the squeezing parameter, x_0 is the (real) displacement, and H_n denotes the Hermite polynomials.

A phase-space representation of this state can be given by the Q function²⁷

$$Q(\alpha) = \langle \alpha | \hat{\rho} | \alpha \rangle, \quad (30)$$

where α is the complex amplitude of a coherent state. This yields

$$Q(\alpha) = \exp(-|\alpha|^2) \left| \sum_{n=0}^{\infty} \frac{(\alpha^*)^n}{\sqrt{n!}} c_n \right|^2. \quad (31)$$

For the case discussed in Section 3, we have to consider^{5,11} a two-mode squeezed state written in the angular-momentum representation, i.e.,

$$|\Psi\rangle = \mathcal{N} \sum_{m=-j}^j c_{j+m} |m\rangle, \quad (32)$$

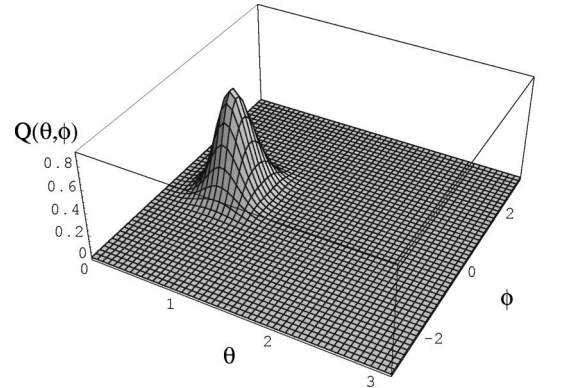
where \mathcal{N} is a normalization factor and the coefficients c_{j+m} are as given in Eq. (29). Since the quantity $x_0^2 + (r^2 - 1)/4r$ represents the mean number of atoms in mode 1, it must be smaller than the total number of atoms N . Furthermore, the atomic coherent-state basis for a system of angular momentum j is defined by²⁸

$$\begin{aligned} |\theta, \phi\rangle &= \sum_{m=-j}^j \mathcal{D}_{m,-j}^{(j)}(\psi = 0, \theta, \phi) |m\rangle \\ &= \sum_{m=-j}^j \binom{2j}{m+j}^{1/2} \left(\sin \frac{\theta}{2} \right)^{j+m} \left(\cos \frac{\theta}{2} \right)^{j-m} \\ &\quad \times \exp(-im\phi) |m\rangle, \end{aligned} \quad (33)$$

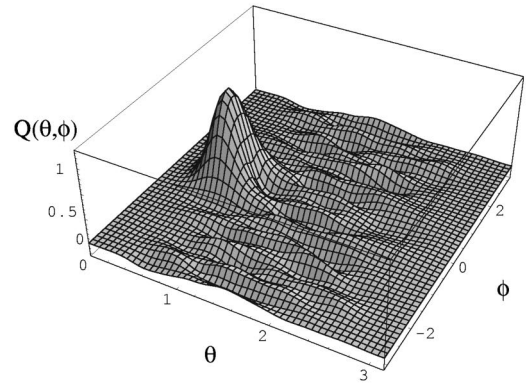
then one can define the Q -quasi-probability distribution analogously to Eq. (30):

$$Q(\theta, \phi) = \langle \theta, \phi | \hat{\rho} | \theta, \phi \rangle. \quad (34)$$

For the state considered in Eq. (32), this equation becomes



(a)



(b)

Fig. 1. Squeezed two-mode state: (a) ideal Q function when the displacement parameter is $x_0 = \sqrt{5}$ and the squeezing parameter is $r = e$, (b) corresponding Q function reconstructed by the method given in Section 3. To obtain this figure we simulated experimental data by adding to each probability w a noise term with a Gaussian distribution whose width was proportional to the ratio between the probability itself and the number of runs for the given parameters.

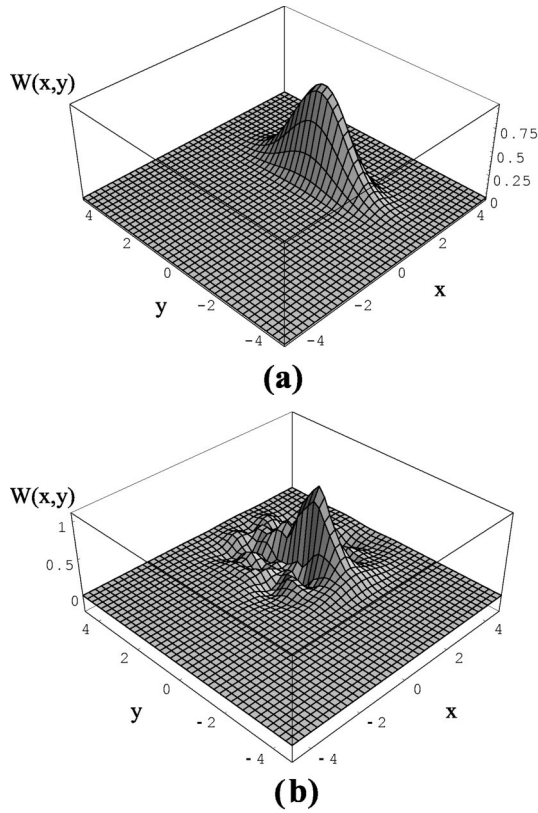


Fig. 2. Squeezed state for the single mode: (a) ideal Wigner function when the displacement parameter is $x_0 = \sqrt{3}$ and the squeezing parameter is $r = e$, (b) corresponding Wigner function reconstructed by the method given in Section 4. The reconstruction parameters are $|\beta| = 1.1$ and $\eta = 0.9$, and 3×10^5 simulated experimental data per each phase have been used (see text).

$$Q(\theta, \phi) = \left| \sum_{m=-j}^j D_{m,-j}^{(j)*}(\psi = 0, \theta, \phi) c_{j+m} \right|^2. \quad (35)$$

This Q function is shown in Fig. 1(a). Figure 1(b) displays the Q function calculated from the reconstructed density-matrix elements. We can see that the method presented in Section 3 is quite accurate, apart from some background noise.

Analogously, in Fig. 2(a) we have plotted the ideal Wigner function²⁷ of Eq. (31), while Fig. 2(b) is its reconstructed version. In this case the statistical error depends on the chosen value of $|\beta|$. For $|\beta|$ values close to zero, the diagonal density-matrix elements can be determined with great precision, whereas the off-diagonal elements strongly fluctuate. The opposite happens when $|\beta|$ is increased. To compensate for the fluctuations the number of measurement events must be increased. Another source of error stems from the truncation of the reconstructed density matrix at the value N_1 .

It is worth comparing the above results with those obtained in the case of a number state. For this purpose, we show in Fig. 3(a) the ideal Wigner function for a number state. In this case the Wigner function becomes negative, displaying the highly nonclassical character of a Fock state. As in the previous figures, in Fig. 3(b) we show the Wigner function obtained by application of Sec-

tion 4's reconstruction method to such a state: The two figures are practically indistinguishable, showing the accuracy of the present method.

Finally, as an instructive comparison we show in Fig. 4 the same Wigner function as in Fig. 2(a), calculated when the state reconstruction takes place with a random-phase relation between probe and condensate. As can be seen, the state becomes randomized and diffused in phase, but its Wigner function remains positive. This figure should be contrasted with Fig. 3. In this case the apparent $U(1)$ symmetry does not pertain to the state²⁹; rather, it is due

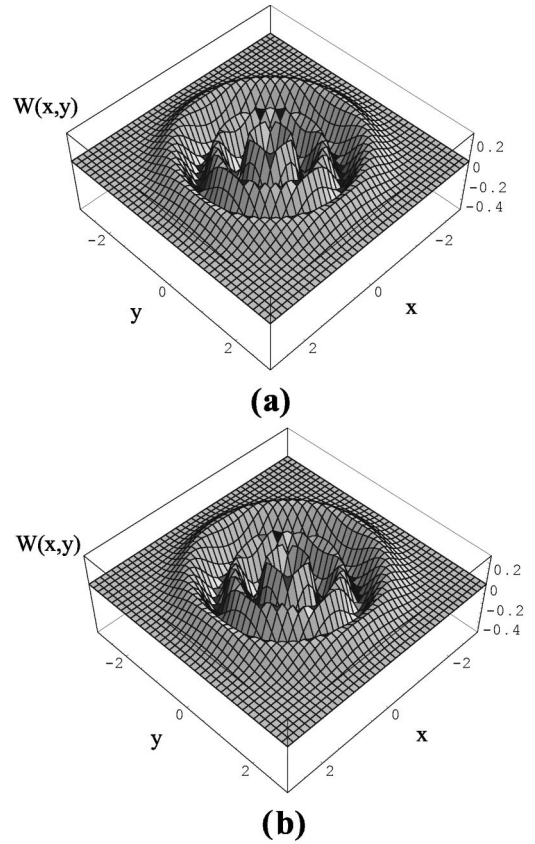


Fig. 3. Number state for the single mode: (a) ideal Wigner function for the Fock state $|n\rangle = |5\rangle$, (b) corresponding Wigner function reconstructed by the method given in Section 4. The reconstruction parameters are $|\beta| = 0.3$ and $\eta = 0.9$, and 3×10^5 simulated experimental data per each phase have been used (see text).

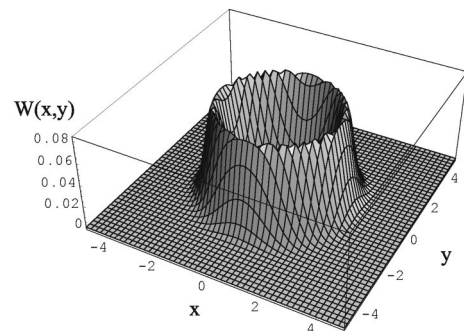


Fig. 4. Squeezed state with a random phase between 0 and 2π . Here a value of the displacement parameter $x_0 = \sqrt{5}$ has been used.

to the measurement method, which implies a preparation of the (same) state at each experimental run.

6. CONCLUSION

To conclude, we have studied, through numerical simulations, the possibilities of a tomographic approach to the quantum state of a Bose–Einstein condensate. We have considered two possible situations: the case in which an atomic reference field is available and that in which it is not available. The corresponding methods turn out to be accurate and robust to detection inefficiency and enable one to distinguish among various possible quantum states of the condensate.

It is worth noting that the techniques studied here allow direct sampling of the density-matrix elements, avoiding any ambiguities in the reconstruction procedure that are due to singularities.³⁰

The key point remains the possibility of having a reference field and/or its state preparation. Furthermore, we note that, to efficiently implement the numerical algorithms, it is necessary to deal with a relatively small number of atoms. Despite these difficulties, we believe that measuring the true density matrix of a condensate is both accessible and a possibility worth considering.

Finally, we would like to remark that the procedures presented here could also be considered for other fields, such as high-energy heavy-ion collisions, where pions can condense as well.³¹

ACKNOWLEDGMENTS

The authors gratefully acknowledge discussions with R. Onofrio. This research has been partially supported by the Istituto Nazionale di Fisica della Materia under the Advanced Research Project “Cat,” by the Ministero dell’Università e della Ricerca Scientifica e Tecnologica, and by the European Union.

M. Fortunato can be reached by e-mail at mauro@camcat.unicam.it.

REFERENCES

1. D. F. Walls and G. J. Milburn, *Quantum Optics* (Springer-Verlag, Berlin, 1994).
2. M. H. Anderson, J. R. Ensher, M. R. Matthews, C. E. Wieman, and E. A. Cornell, “Observation of Bose–Einstein condensation in a dilute atomic vapor,” *Science* **269**, 198–201 (1995); K. B. Davies, M.-O. Mewes, M. R. Andrews, N. J. van Druten, D. S. Durfee, D. M. Kurn, and W. Ketterle, “Bose–Einstein condensation in a gas of sodium atoms,” *Phys. Rev. Lett.* **75**, 3969–3973 (1995); C. C. Bradley, C. A. Sackett, J. J. Tollett, and R. G. Hulet, “Evidence of Bose–Einstein condensation in an atomic gas with attractive interactions,” *Phys. Rev. Lett.* **75**, 1687–1690 (1995).
3. M. R. Andrews, C. G. Townsend, H. J. Miesner, D. S. Durfee, D. M. Kurn, and W. Ketterle, “Observation of interference between two Bose–Einstein condensates,” *Science* **275**, 637–641 (1997).
4. W. Ketterle and H. J. Miesner, “Coherence properties of Bose–Einstein condensates and atom lasers,” *Phys. Rev. A* **56**, 3291–3293 (1997).
5. M. Lewenstein and L. You, “Quantum phase diffusion of a Bose–Einstein condensate,” *Phys. Rev. Lett.* **77**, 3489–3493 (1996); M. J. Steel and M. J. Collett, “Quantum state of two trapped Bose–Einstein condensates with a Josephson coupling,” *Phys. Rev. A* **57**, 2920–2930 (1998).
6. H. Zeng, W. Zhang, and F. Lin, “Nonclassical Bose–Einstein condensate,” *Phys. Rev. A* **52**, 2155–2160 (1995).
7. J. Ruostekoski and J. Javanainen, “Quantum field theory of cooperative atom response: low light intensity,” *Phys. Rev. A* **55**, 513–526 (1997); E. A. Burt, R. W. Ghrist, C. J. Myatt, M. J. Holland, E. A. Cornell, and C. E. Wieman, “Coherence, correlations and collisions: what one learns about Bose–Einstein condensates from their decay,” *Phys. Rev. Lett.* **79**, 337–340 (1997).
8. See, e.g., U. Leonhardt, *Measuring the Quantum State of Light* (Cambridge U. Press, Cambridge, UK, 1997); *J. Mod. Opt.* **44**, 11/12, special issue on quantum state preparation and measurement.
9. S. Mancini and P. Tombesi, “Quantum state reconstruction of a Bose–Einstein condensate,” *Europhys. Lett.* **40**, 351–355 (1997).
10. E. L. Bolda, S. M. Tan, and D. F. Walls, “Reconstruction of the joint state of a two-mode Bose–Einstein condensate,” *Phys. Rev. Lett.* **79**, 4719–4723 (1997); R. Walsler, “Measuring the state of a bosonic two-mode quantum field,” *Phys. Rev. Lett.* **79**, 4724–4727 (1997).
11. E. L. Bolda, S. M. Tan, and D. F. Walls, “Measuring the quantum state of a Bose–Einstein condensate,” *Phys. Rev. A* **57**, 4686–4694 (1998).
12. D. T. Smithey, M. Beck, M. G. Raymer, and A. Faridani, “Measurement of the Wigner distribution and the density matrix of a light mode using optical homodyne tomography: application to squeezed states and the vacuum,” *Phys. Rev. Lett.* **70**, 1244–1247 (1993).
13. R. Spreeuw, T. Pfau, U. Janicke, and M. Wilkens, “Laser-like scheme for atomic matter waves,” *Europhys. Lett.* **32**, 469–474 (1995); M. Holland, K. Burnett, C. Gardiner, J. I. Cirac, and P. Zoller, “Theory of an atom laser,” *Phys. Rev. A* **54**, 1757–1760 (1996); H. Wiseman, A. M. Martins, and D. F. Walls, “An atom laser based on evaporative cooling,” *Quantum Semiclass. Opt.* **8**, 737–753 (1996); H. Steck, M. Naraschewski, and H. Wallis, “Output of a pulsed atom laser,” *Phys. Rev. Lett.* **80**, 1–5 (1998); J. Schneider and A. Schenzle, “Output from an atom laser: theory vs. experiment,” *Appl. Phys. B* **69**, 353–356 (1999); I. Bloch, T. W. Hänsch, and T. Esslinger, “Atom laser with a cw output coupler,” *Phys. Rev. Lett.* **82**, 3008–3011 (1999).
14. J. A. Dunningham and K. Burnett, “Phase standard for Bose–Einstein condensates,” *Phys. Rev. Lett.* **82**, 3729–3733 (1999).
15. S. Mancini, V. I. Man’ko, and P. Tombesi, “Different realizations of the tomography principle in quantum state measurement,” *J. Mod. Opt.* **44**, 2281–2292 (1997).
16. G. M. D’Ariano, “Group theoretical quantum tomography,” *Acta Phys. Slovaca* **49**, 513–522 (1999).
17. E. P. Wigner, *Perspectives in Quantum Theory*, W. Yourgrau and A. van der Merwe, eds. (Dover, New York, 1979).
18. P. Berman, ed., *Atom Interferometry* (Academic, New York, 1997); M.-O. Mewes, M. R. Andrews, D. M. Kurn, D. S. Durfee, C. G. Townsend, and W. Ketterle, “Output coupler for Bose–Einstein condensed atoms,” *Phys. Rev. Lett.* **78**, 582–585 (1997); H. Hinderthur, A. Pautz, F. Ruschewitz, K. Sengstock, and W. Ertmer, “Atomic interferometry with polarizing beam splitters,” *Phys. Rev. A* **57**, 4730–4735 (1998).
19. L. C. Biedenharn and H. Van Dam, eds., *Quantum Theory of Angular Momentum* (Academic, New York, 1965).
20. V. V. Dodonov and V. I. Man’ko, “Positive distribution description for spin states,” *Phys. Lett. A* **229**, 335–339 (1997).
21. V. I. Man’ko and O. V. Man’ko, “Spin state tomography,” *Zh. Eksp. Teor. Fiz.* **112**, 796–800 (1997) [*JETP* **85**, 430–434 (1997)].
22. S. Wallentowitz and W. Vogel, “Unbalanced homodyning for quantum state measurements,” *Phys. Rev. A* **53**, 4528–4533 (1996); K. Banaszek and K. Wodkiewicz, “Direct probing of quantum phase space by photon counting,” *Phys.*

- Rev. Lett. **76**, 4344–4347 (1996); S. Mancini, P. Tombesi, and V. I. Man'ko, "Density matrix from photon number tomography," *Europhys. Lett.* **37**, 79–83 (1997).
23. T. Opatrny and D. G. Welsch, "Density matrix reconstruction by unbalanced homodyning," *Phys. Rev. A* **55**, 1462–1465 (1997).
 24. See, e.g., D. J. S. Robinson, *A Course in Linear Algebra with Applications* (World Scientific, Singapore, 1991); W. T. Vetterling, S. A. Teukolsky, W. H. Press, and B. P. Flannery, *Numerical Recipes* (Cambridge U. Press, Cambridge, UK, 1985).
 25. M. O. Scully and W. E. Lamb, "Quantum theory of optical maser. III. Theory of photoelectron counting statistics," *Phys. Rev.* **179**, 368–374 (1969).
 26. K. Vogel and W. Schleich, "More on interference in phase space," in *Fundamental Systems in Quantum Optics*, J. Dalibard, J.-M. Raimond, and J. Zinn-Justin, eds. (North-Holland, Amsterdam, 1992), pp. 713–765.
 27. M. Hillery, R. F. O'Connell, M. O. Scully, and E. P. Wigner, "Distribution functions in physics: fundamentals," *Phys. Rep.* **106**, 121–167 (1986). The Wigner function is a more refined picture of the quantum state in phase space and is particularly suited to display quantum characters of the state. In simple words, the Q function is a smoothed version of the Wigner function.
 28. F. T. Arecchi, E. Courtens, R. Gilmore, and H. Thomas, "Atomic coherent states in quantum optics," *Phys. Rev. A* **6**, 2211–2237 (1972); G. S. Agarwal, "Relation between atomic coherent representation, state multipoles and generalized phase space distributions," *Phys. Rev. A* **24**, 2889–2896 (1981).
 29. D. Forster, *Hydrodynamic Fluctuations, Broken Symmetry, and Correlation Functions* (Benjamin, New York, 1975); K. Huang, *Statistical Mechanics*, 2nd ed. (Wiley, New York, 1987).
 30. G. M. D'Ariano, U. Leonhardt, and H. Paul, "Homodyne detection of the density matrix of the radiation field," *Phys. Rev. A* **52**, R1801–R1804 (1995).
 31. P. Braun-Munzinger, H. J. Specht, R. Stock, and H. Stocker, eds., *Quark Matter*, *Nucl. Phys. A* **610**, 1c–565c (1996); T. Csorgo, P. Levai, and J. Zimanyi, eds., *Strangeness in Hadronic Matter*, *Heavy Ion Phys.* **4**, 1–464 (1996); S. Pratt, "Pion lasers from high-energy collisions," *Phys. Lett. B* **301**, 159–164 (1993).